Journal of Molecular Liquids 428 (2025) 127502

Contents lists available at ScienceDirect

Journal of Molecular Liquids

journal homepage: www.elsevier.com/locate/molliq

Lubricant properties of a polyalphaolefin oil additivated with zirconia and ceria-zirconia nanoparticles

María J.G. Guimarey [a,*], Arturo Castro Currás [a], José M. Liñeira Del Río [a,b], María J.P. Comuñas [a]

[a] Laboratory of Thermophysical and Tribological Properties, Nafomat Group, Department of Applied Physics, Faculty of Physics, and Institute of Materials (iMATUS), University of Santiago de Compostela, Santiago de Compostela, 15782, Spain
[b] Unidade de Tribologia, Vibraçoes e Manutençao Industrial, INEGI, Universidade do Porto, Porto 4200-465, Portugal

ARTICLE INFO

Keywords:
Zirconia
Ceria-zirconia
Polyalphaolefin
Viscosity
Friction coefficient
Wear

ABSTRACT

In this work zirconia (ZrO_2) and hybrid ceria-zirconia (CeO_2-ZrO_2) nanoparticles are used for the first time as lubricant additives of the PAO8 base oil (low-viscosity polyalphaolefin oil) at concentrations from 0.05 wt% to 0.20 wt%. Thermophysical properties of the eight formulated nanolubricants were experimentally determined observing that the presence of these nanoadiditves not significantly alter the volumetric behaviour of neat PAO8. On the contrary, the presence of CeO_2-ZrO_2 in formulation increases the viscosity of the base oil by up to 13 %. Tribological tests were performed under pure sliding conditions at 393.15 K at a load of 20 N using a ball-on-three-pin rotational tribometer. Moreover, the wear was quantified with a 3D optical profilometer. Nanolubricants with zirconia nanoparticles exhibited superior characteristics in terms of stability, antifriction and anti-wear properties than those formulated with hybrid ceria-zirconia nanoparticles. The best tribological behaviour was obtained with 0.05 wt% ZrO_2, thus reductions of 13 % in friction coefficient and of 73 % in the worn area were obtained. The results obtained have been compared with those previously reported for the same base oil (PAO8) and other types of nanoadditives. Finally, surface roughness analysis, Raman microscopy and SEM-EDX were used to analyse the wear mechanism produced by zirconia and hybrid ceria-zirconia nanoparticles.

1. Introduction

Electric vehicles (EVs) offer a sustainable and eco-friendly alternative to internal combustion vehicles, but their operating conditions—high speeds, heavy loads, elevated temperatures, and electrical currents—place unique demands on their mechanical components (e.g., motors, transmissions, wheel bearings, and suspensions) [1–3]. Consequently, minimizing friction in electric drivetrains is crucial to enhance efficiency and achieve energy savings.

The development of transmission fluids for EVs involves close collaboration among lubricant manufacturers, automotive engineers, and researchers. Advances in lubricant technology not only improve overall vehicle efficiency and reliability but also ensure compatibility with the specific materials used in EV components (seals, gaskets, various metals) while providing necessary electrical insulation, thermal stability, and low viscosity to reduce motor torque and enhance cooling performance [2–7]. Lubricants typically comprise 80–90 % base oil and 10–20 % additives, so carefully selecting both components is essential to meet these diverse performance requirements. In response to growing environmental concerns associated with petroleum-derived products, synthetic base oils—particularly polyalphaolefins (PAOs)—have become prevalent due to their high thermal stability, oxidation resistance, and dielectric properties. PAOs are classified by their kinematic viscosities at 373.15 K, typically ranging from 2 to 100 cSt [8,9].

Recent studies have demonstrated that incorporating nanomaterials into PAOs can significantly enhance their tribological properties by mechanisms such as rolling effects, protective film formation, repair, and polishing [10–13]. Most of the published work in this area has focused on metal-containing nanomaterials, including their oxides and sulphides [13–15]. For instance, Kalin et al. [16] showed that PAO6 additivated with MoS_2 multi-wall nanotubes reduced friction and wear by up to 2 and 9 times, respectively, compared to neat PAO6. Other studies have similarly reported significant improvements using WS_2, Ni, ZnO, and other nanoparticles [12,17–23].

* Corresponding author.
E-mail address: mariajesus.guimarey@usc.es (M.J.G. Guimarey).

https://doi.org/10.1016/j.molliq.2025.127502
Received 25 November 2024; Received in revised form 13 March 2025; Accepted 1 April 2025
Available online 2 April 2025

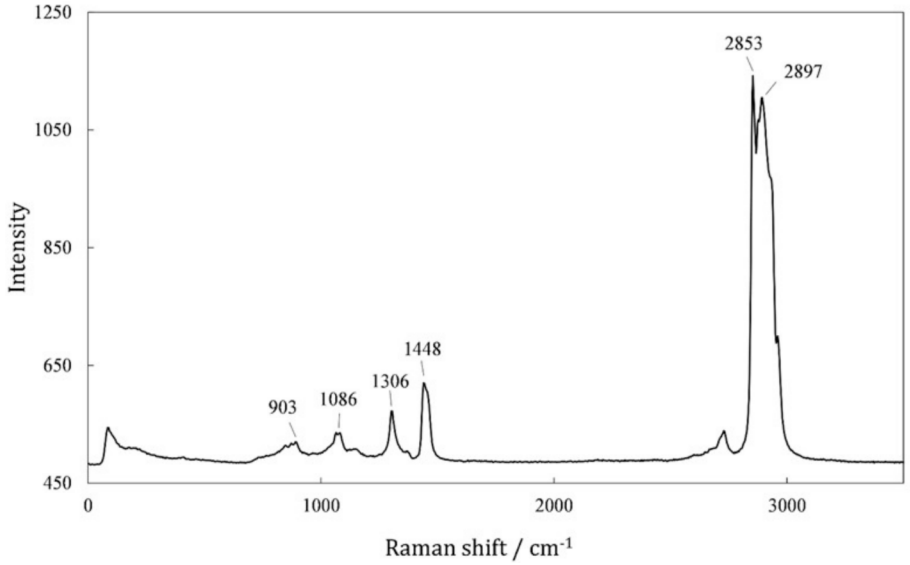

Fig. 1. Raman spectrum of PAO8 base oil.

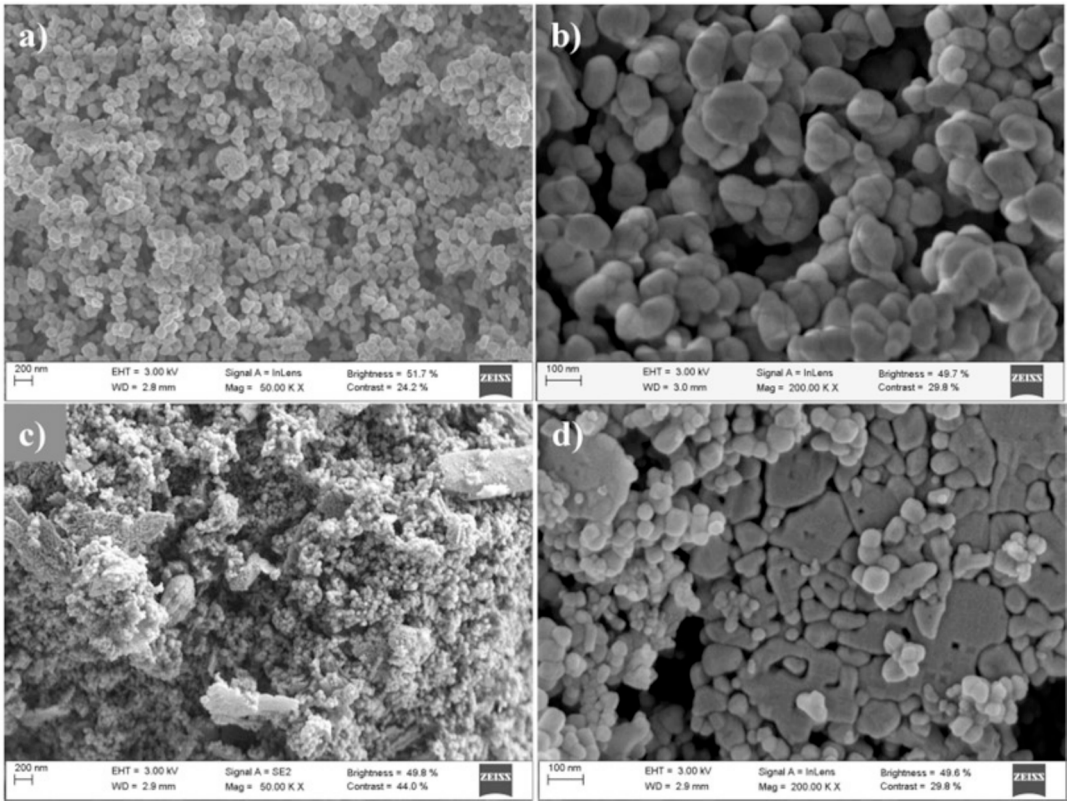

Fig. 2. SEM images of ZrO_2 at a) 50 K X and b) 200 K X and CeO_2-ZrO_2 at c) 50 K X and d) 200 K X.

Within this context, the present study is part of a broader research project focused on the thermophysical and tribological properties of nanolubricants for EVs. For transmission fluids in EVs, low-viscosity base oils are essential; thus, we have selected PAO8 (kinematic viscosity around 8 mm^2/s at 373.15 K). While previous works have explored the effects of ZrO_2 nanoparticles in PAO6 and PAO4 [6,24–27], there is a notable gap regarding the use of CeO_2/ZrO_2 hybrid nanoparticles in PAO formulations. Only Philip et al. [28] have examined the surface morphology of CeO_2 and Ce-Zr hybrid nanoparticles for potential lubricant applications, and studies on CeO_2 as an additive in PAOs have indicated that CeO_2-based composites can enhance tribological performance [29–31].

The novelty of our work lies in the first-time use of ZrO_2 and CeO_2/ZrO_2 hybrid nanoparticles as additives in PAO8. This study aims to complete the evaluation of various nanomaterials as additives in polyalphaolefins, potentially leading to optimized formulations that offer superior performance in EV transmission systems.

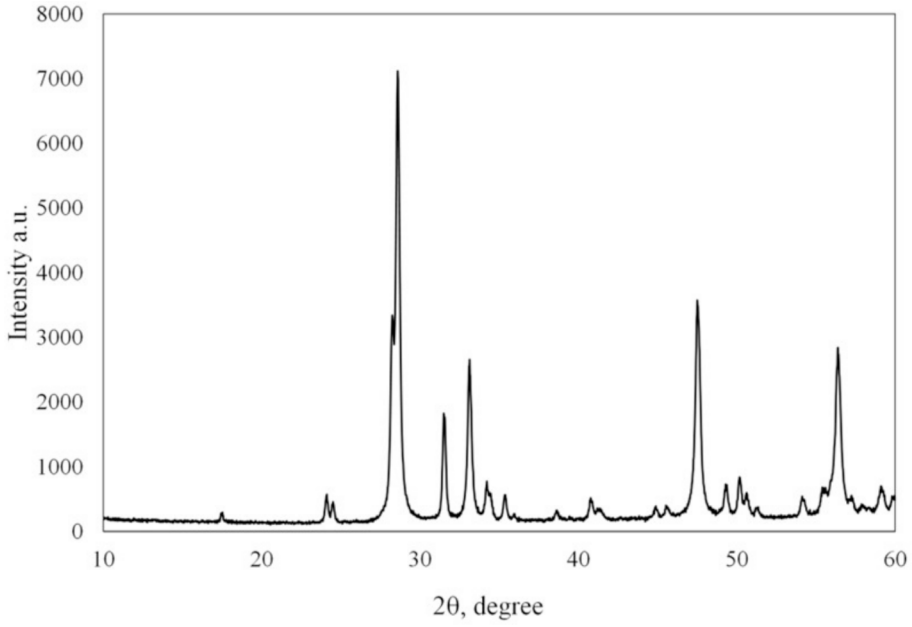

Fig. 3. X-ray patterns of the nanopowder of CeO_2-ZrO_2.

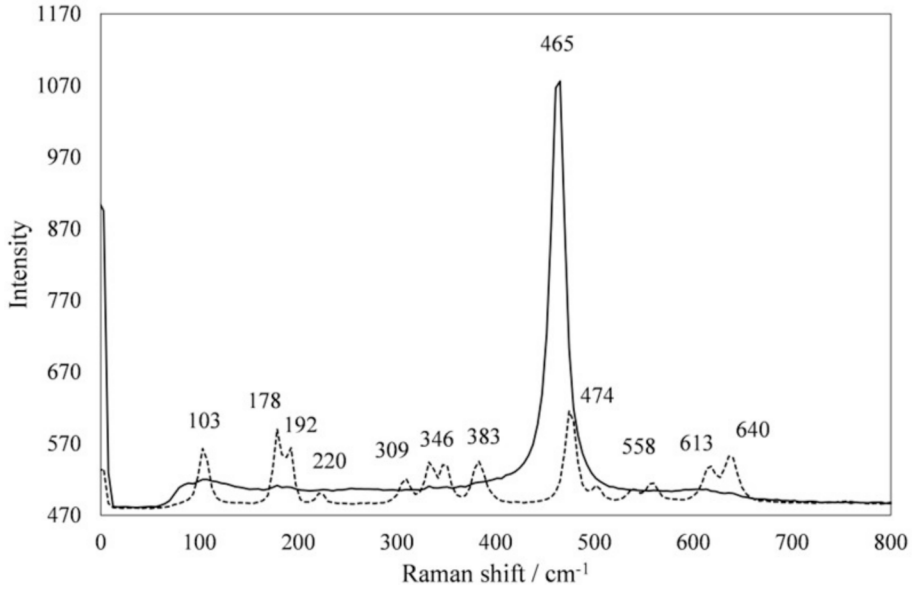

Fig. 4. Raman spectra of ZrO_2 (dashed line) and CeO_2-ZrO_2 (solid line).

2. Materials

2.1. Nanoadditives and base oil characterisation

A low viscosity polyalphaolefin (PAO8) supplied by Repsol, with a viscosity index of 138, was used as base oil to prepare the nanolubricants. Density and viscosity of PAO8 over the temperature interval 278.15 to 373.15 K are reported in Tables S1 and S2 in the Supplementary Material. PAO8 dynamic viscosity ranges from 6.26 to 253.14 mPa s and density from 0.7794 to 0.8375 g cm^{-3}, over all the temperature intervals. Raman spectrum of PAO8 oil, shown in Fig. 1, was performed with a WITec alpha300R+ confocal Raman microscopy at a wavelength of 532 nm. An intense broad band was detected around 2800–3000 cm^{-1} with peaks at 2853 and 2897 cm^{-1} assignable to C–H stretching [32]. The peaks at 1306 and 1448 cm^{-1} correspond to the $\delta(CH_2)$ and $\delta(CH_3)$ vibrations, respectively [32], and the peaks at 903 and 1086 cm^{-1} can be attributed to the vibrations of the aliphatic ν(C–C) chains [33].

ZrO_2 nanoparticles (Iolitec) and CeO_2-ZrO_2 nanocomposite (US Research Nanomaterials, Inc.) were used as lubricant additives. The size and morphology of ZrO_2 and CeO_2-ZrO_2 nanopowders were analysed by scanning electron microscopy (SEM). As shown in Fig. 2, SEM images reveal that the two types of nanoparticles have a spherical shape and the difference in size between ZrO_2 (30–60 nm) and CeO_2-ZrO_2 (15 nm) can be distinguished. The X-ray patterns of ZrO_2 nanopowder is reported in a previous work [24]. EDX spectrum and elemental mapping of CeO_2-ZrO_2 nanoadditives are shown in Fig. S1 in the Supplementary Material. Elemental mapping (Fig. S1 a, b and c) reveals a homogeneous distribution on the nanoadditives. In particular, the distribution of elements: Ce, O and Zr, was 27.7, 20.2 and 14.1 wt%, respectively. As can be seen

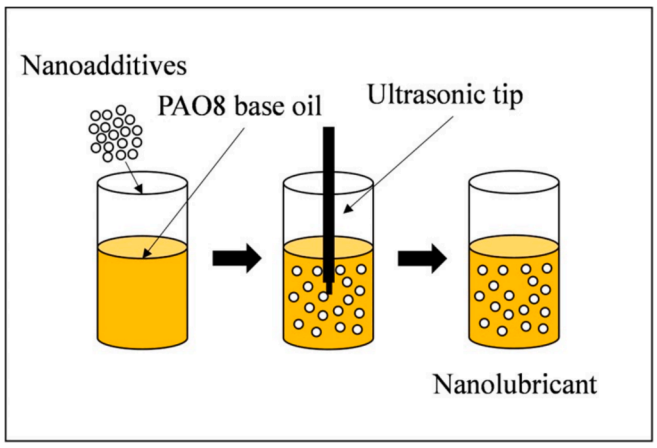

Fig. 5. Scheme of the procedure used for the nanolubricants formulation.

from Fig. 3, the main phase of CeO_2-ZrO_2 nanopowders is the typical diffraction peaks of $Ce_{0.02}O_2Zr_{0.98}$ cubic phase at $2\theta = 28.57°$, 33.10°, 47.50°, and 56.36° due to (111), (200), (220) and (311) planes, respectively [34].

To complete the characterisation of the nanopowders, Raman spectroscopy was employed using the confocal Raman microscope (WITec alpha300R+) with a 532 nm excitation laser. Fig. 4 shows the Raman spectra with the characteristic bands for both nanoparticles. In the ZrO_2 spectrum, several peaks are observed centred at 103, 178, 192, 309, 346, 383, 474, 558, 618 and 640 cm^{-1}. The peaks of highest intensity are placed at 103, 178 and 474 cm^{-1}, which confirm the monoclinic crystal structure of ZrO_2 nanoparticles [35]. In the case of the Raman spectrum of CeO_2-ZrO_2 hybrid nanoparticles, characteristic bands are observed around 103, 465 and 618 cm^{-1}. The strongest peak at 465 cm^{-1} corresponds to cerium oxide [36], while the weak peaks at 103 and 618 cm^{-1} are due to ZrO_2.

2.2. Nanolubricants preparation

Eight PAO8-based nanolubricants were prepared, four of them with ZrO_2 and four with CeO_2-ZrO_2 hybrid nanoparticles, in both cases the nanoadditive mass concentrations were 0.05, 0.075, 0.10 and 0.20 wt% (Fig. 5). The addition of the powdered nanoadditives to the polyalphaolefin oil base was controlled with a Sartorius MC 210P microbalance. To ensure the homogenisation of nanoaditives, a Bandelin Sonopuls HD2200 ultrasonic tip was used at fixed power (15 %) and frequency (37 kHz) for 30 min. An ice-water bath was used to avoid overheating of nanolubricants during the sonication process.

3. Experimental techniques

Density and dynamic viscosity of the nanolubricants were measured from 278.15 to 373.15 K with 5 K step, at atmospheric pressure with a rotational Stabinger viscometer SVM 3000 from Anton Paar (Graz, Austria). The automated viscometer is based on a modified Couette principle, which includes a vibrating tube densimeter. In addition, this equipment was also used to determine the viscosity index (VI) according to ASTM D2270 and ISO 2909 standards. This device has previously been described in detail [37]. The expanded uncertainties (k = 2) are 0.0005 $g{\cdot}cm^{-3}$ and 1 % for density and dynamic viscosity, respectively. For the temperature in the range from 288.15 to 378.15 K the expanded uncertainty is 0.02 K and outside this range 0.05 K.

An Anton Paar MCR 302 rheometer equipped with a T-PTD 200 tribology cell heated by a Peltier hood HPTD200 was used to experimental determine the friction coefficient. The test consists in a pure-sliding rotational motion between a diameter 12.7 mm ball and 6 mm three pins, with a maximum contact pressure of 1.1 GPa. The friction tests last approximately one hour. The test scheme and the conditions are shown in Fig. 6. The specimens used were polished AISI 52100 (100Cr6) steel (Ra = 20 nm for the ball and Ra = 50 nm for the pins) with hardness of 62–66 HRC. Balls and pins were cleaned with a stream of hexane and dried with air before the tests. Samples were fully submerged by adding around 1 mL of lubricant. The contact pressure and the very low surface separation are typical of the severe boundary lubrication met in automotive applications, such as gears or bearings [2,38].

To analyse the wear produced on the pins lubricated with the neat PAO8 and with the PAO8/ZrO_2 and PAO8/CeO_2-ZrO_2 nanolubricants a Sensofar S Neox 3D optical profilometer was used. Specifically, the following wear parameters were determined: diameter (WSD), depth, (WTD), area (A) and volume (V) of the wear track (Fig. 7). The

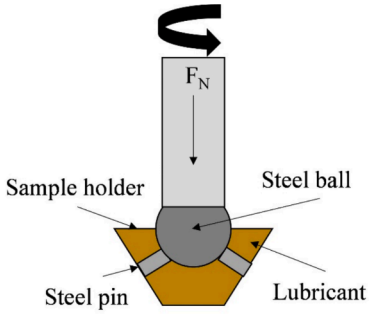

Experimental conditions	
Load (N)	20
Maximum contact pressure (GPa)	1.1
Sliding speed (m s^{-1})	0.1
Sliding distance (m)	340
Temperature (K)	393.15

Fig. 6. Tribological test scheme and experimental conditions.

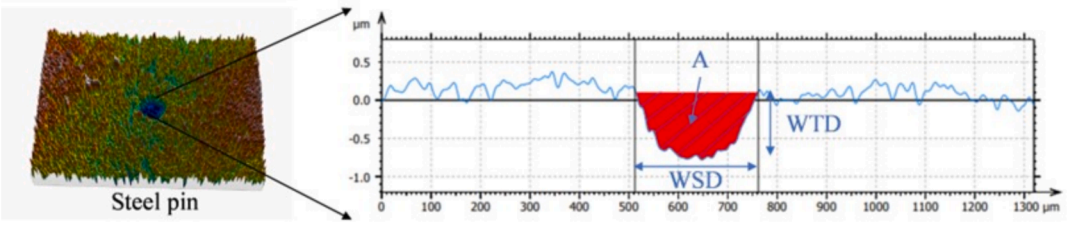

Fig. 7. Wear parameters measured using a Sensofar S Neox 3D optical profilometer.

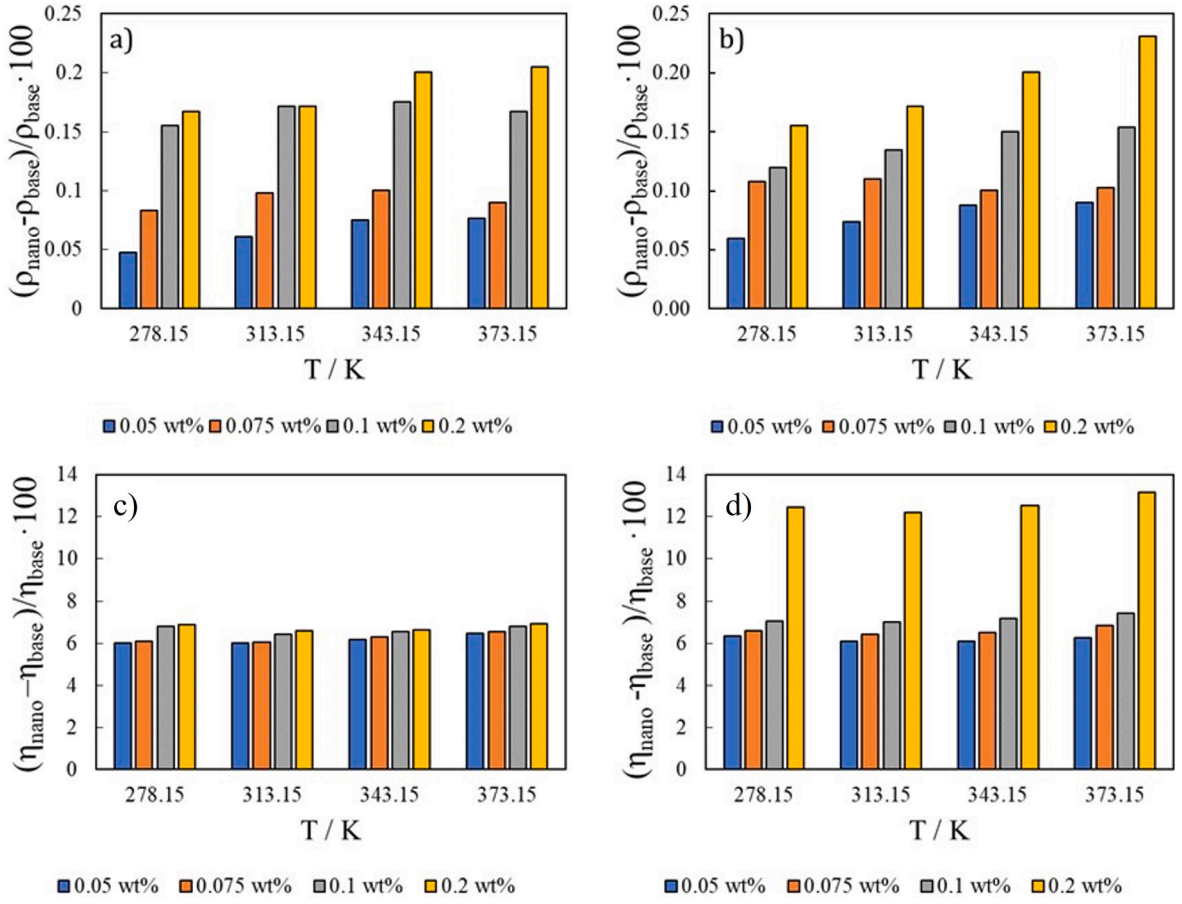

Fig. 8. Density (ρ) and dynamic viscosity (η) variation of the nanolubricants due to the presence of ZrO_2 (a, c) and CeO_2-ZrO_2 (b, d) nanoparticles.

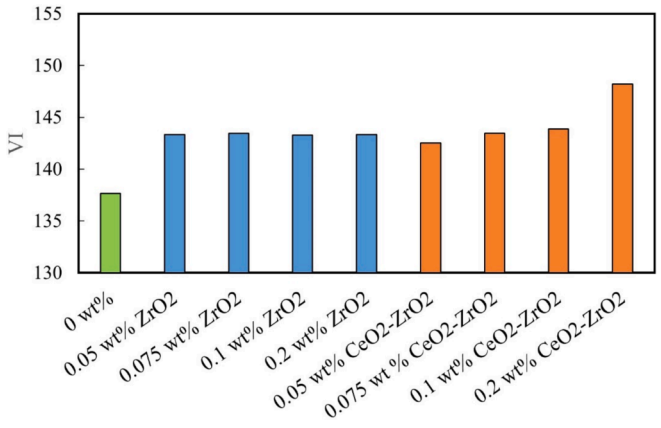

Fig. 9. Viscosity index (VI) values for PAO8 base oil (0 wt%) [23] and for all nanolubricants.

measurements were performed using the confocal mode of the optical profilometer with a 10X objective. In addition, the roughness (Ra) of the worn area of the pins was also determined and compared with the roughness of the unworn samples according to ISO4287 (Gaussian filter with a cut-off wavelength of 0.08 mm). This analysis is useful to describe the possible anti-wear mechanism of nanoadditives. To complete the anti-wear analysis of the nanolubricants, Raman mapping of the worn surfaces was performed with the WITec alpha300R+ confocal equipment, which provides information on the distribution of the nanolubricant components (PAO8, and ZrO_2 or CeO_2-ZrO_2 nanoparticles) in the wear tracks, and on the possible tribological mechanisms that can occur. To further analyze the effect of the additives in the worn pin surfaces, SEM micrographs of the PAO8 base oil and its formulated lubricants (PAO8 + 0.05 wt% ZrO_2 and PAO8 + 0.1 wt% CeO_2-ZrO_2) were obtained with a Zeiss Ultraplus Field Emission Scanning Electron Microscope, FESEM, at two magnifications (500X and 5000X).

4. Results and discussion

The density values obtained for the PAO8 neat oil and for all the PAO8/ZrO_2 and PAO8/CeO_2-ZrO_2 nanolubricants are presented in Table S1 in the Supplementary Material. Fig. 8a and 8b shows the density variation with the concentration for both ZrO_2 and CeO_2-ZrO_2-based nanolubricants. As can be observed, the presence of ZrO_2 or CeO_2-ZrO_2 nanoparticles not significantly alter the volumetric behaviour of the neat base oil (PAO8). Thus, density relative variations less than 0.3 % are observed with the two types of nanoparticles. This fact agrees with

Table 1
Average friction coefficients (COF), diameter (WSD), depth (WTD) and area (A) of the worn tracks lubricated with neat PAO8, PAO8/ZrO_2 and PAO8/CeO_2-ZrO_2 nanolubricants and their standard deviations (σ).

Lubricant	COF	σ	WSD/μm	σ /μm	WTD/μm	σ/μm	A/10^2μm^2	σ/10^2μm^2
PAO8 [22]	0.1392	0.0021	392	14	2.35	0.17	6.05	0.52
+0.05 wt% ZrO_2	0.1212	0.0021	248	9	0.81	0.15	1.46	0.36
+0.075 wt% ZrO_2	0.1224	0.0025	272	10	1.01	0.10	2.45	0.49
+0.1 wt% ZrO_2	0.1296	0.0026	296	5	1.44	0.09	3.27	0.24
+0.2 wt% ZrO_2	0.1404	0.0038	373	3	1.89	0.10	5.08	0.22
+0.05 wt% CeO_2-ZrO_2	0.1345	0.0037	387	5	2.11	0.21	6.37	0.62
+0.075 wt% CeO_2-ZrO_2	0.1218	0.0025	302	15	1.14	0.19	2.97	0.67
+0.1 wt% CeO_2-ZrO_2	0.1314	0.0024	270	15	1.13	0.26	2.31	0.41
+0.2 wt% CeO_2-ZrO_2	0.1471	0.0040	381	14	2.16	0.32	6.30	0.95

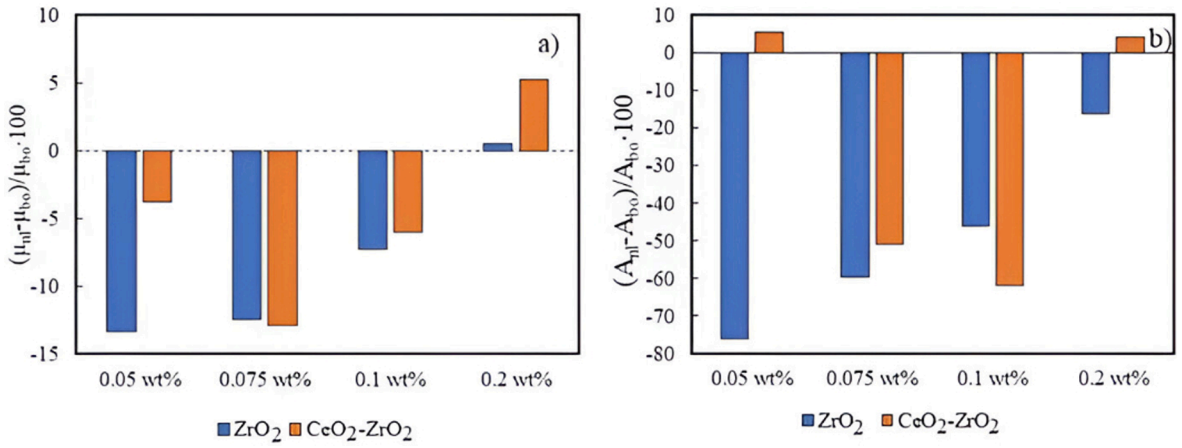

Fig. 10. Relative variation of the friction coefficient (a) and wear area (b) of nanolubricants with respect to the base oil as a function of nanoparticle concentration.

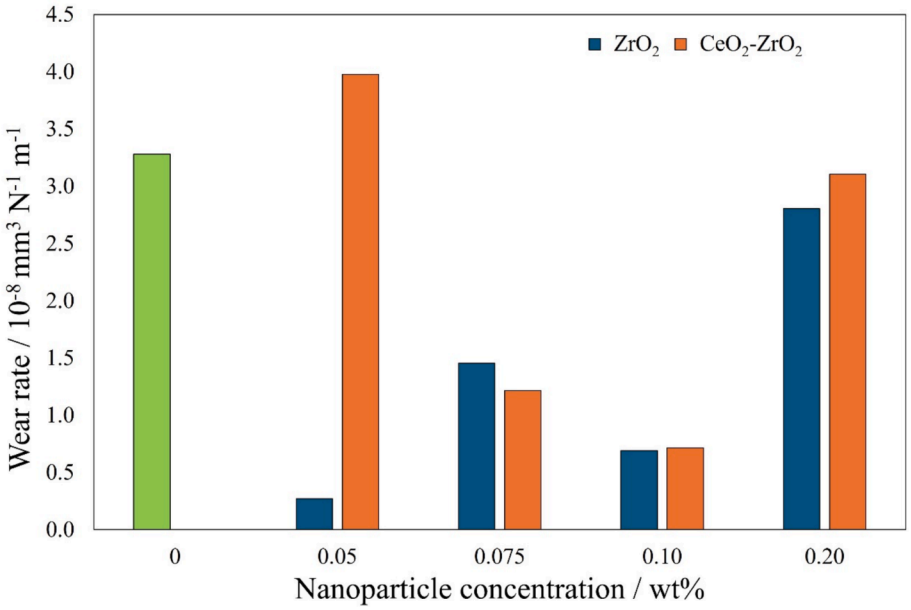

Fig. 11. Steel pins ' wear rate (W) lubricated with PAO8 (0 wt%) and nanolubricants containing ZrO_2 and CeO_2-ZrO_2 at different concentrations (0.05, 0.075, 0.10, and 0.20 wt%).

previous results for PAO40/ZnO-OA [21].

Table S2 gathered the dynamic viscosity values for all nanolubricants as a function of the temperature and nanoparticle concentration. As can be seen in Fig. 8c and 8d, a 0.2 wt% of CeO_2-ZrO_2 produce an increase in the viscosity of around 13 % with respect to the neat PAO8. For the other concentrations of CeO_2-ZrO_2 and for all PAO8/ZrO_2 nanolubricants, the increase in viscosity is in the range of 6–8 %. The viscosity increase due to the presence of the nanoparticles is important for the industrial use of the nanolubricant, as it could lead to an increase in the machine's energy consumption [39]. In the case of EVs, low viscosity means higher fluidity which facilitates oil supply to the contact zone and dissipates heat by reducing viscous heating at high rpm [2].

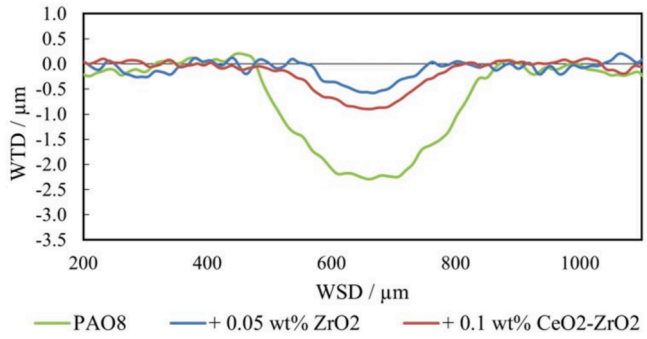

Fig. 12. Cross-sectional wear profile for base oil and for optimal nanoparticle concentrations.

As Fig. 9 shows, the presence of ZrO_2 nanoparticles increases the VI from 138 (neat PAO8) to 143 (for all the ZrO_2 concentrations), which means an increase of 4 %. When CeO_2- ZrO_2 nanoparticles are used, we also observe values of 143–144 (for concentrations from 0.05 to 0.1 wt %) and a higher value of 148 (for the 0.2 wt% concentration). Thus, it can be concluded that the presence of the ZrO_2 and CeO_2- ZrO_2 nanoparticles slightly modifies the viscosity behaviour of the neat PAO8 with temperature.

The results of the friction tests and wear analysis carried out with the tribological cell T-PTD 200 and with the Sensofar S Neox 3D optical profilometer, respectively, for PAO8/ ZrO_2 and PAO8/CeO_2-ZrO_2 at concentrations of 0.05, 0.075, 0.1 and 0.2 wt%, are shown in Table 1. As can be seen in Fig. 10a the best anti-friction (AF) behaviour occurs with the nanolubricants of PAO8 + 0.05 wt% ZrO_2 and PAO8 + 0.075 wt% CeO_2-ZrO_2 with an average friction coefficient value of 0.1212 and 0.1218, respectively. We must remark that a value of 0.1392 has been found for the neat PAO8 in previous works [22]. Therefore, it is observed that the presence of nanoparticles results in a reduction of the friction coefficient of around 13 % for the optimal concentrations of ZrO_2 and CeO_2-ZrO_2. In general, ZrO_2 nanolubricants show better AF behaviour than CeO_2-ZrO_2 nanolubricants. It is important to mention that for concentrations of 0.2 wt% of the two nanoparticles the friction between the ball and the pins is higher than for the neat base oil. This fact may be due to nanoparticles agglomeration when exceeding the optimum concentration. Thus, the mechanical entrapment theory of Chiñas and Spikes [40], states that nanoparticles with a size smaller than or similar to the film thickness of the lubricant, penetrate the contact zone and deposit on it.

Regarding the anti-wear capacity (AW), the results obtained on the worn pins after contact with the ball (Table 1) show that the dispersions of ZrO_2 have a greater influence in improving the anti-wear resistance of PAO8 than those of CeO_2-ZrO_2. Fig. 10b reveals the highest AW capacity of PAO8 + 0.05 wt% ZrO_2, achieving almost 76 % less worn area. It is important to note that for CeO_2-ZrO_2 nanoparticles, the concentration of 0.1 wt% is the one with the greatest (around 60 % of reduction) anti-wear capacity (Fig. 10b).

The wear rate was determined from the wear volume measurements obtained from the steel pins using the following equation [41,42]:

$$W = \frac{\Delta V}{F_n S} \tag{1}$$

where W is the specific wear rate ($mm^3\ N^{-1}{\cdot}m^{-1}$), ΔV represents the wear volume loss (mm^3), F_n is the applied normal load (N), and S corresponds to the sliding distance (m). This method enables a quantitative comparison of the wear performance across different lubricant formulations under severe boundary lubrication conditions.

As shown in Fig. 11, the base oil (PAO8) exhibits almost the highest wear rate, highlighting its limited antiwear capability. The incorporation of nanoparticles significantly reduces wear in all tested concentrations except for the 0.05 wt% CeO_2-ZrO_2 nanolubricant, which shows an unexpected increase in wear rate compared to the other nanolubricants. The best wear reduction is observed at 0.05 wt% for ZrO_2 and 0.10 wt% for CeO_2-ZrO_2 nanolubricant, suggesting an optimal nanoparticle concentration for effective wear protection.

The anomalous behaviour at 0.05 % CeO_2-ZrO_2 could be attributed to insufficient nanoparticle availability to form a stable and protective tribofilm. At very low concentrations, nanoparticles may not fully cover the contact surface or may not effectively contribute to the rolling/sliding mechanism, leading to a lubrication regime closer to that of the base oil. Additionally, particle agglomeration at low concentrations could reduce the dispersion stability, preventing an even distribution within the lubricant film and leading to localised asperity contact and increased wear. Similar trends have been reported in nanoparticle-based lubrication studies [43,44], where an optimal concentration range exists, beyond which either insufficient coverage or excessive particle agglomeration can diminish lubrication efficiency.

Fig. 12 shows the extracted cross-sectional wear profiles for the neat PAO8 and for the nanolubricants with the highest anti-wear capacity concentrations (0.05 wt% of ZrO_2 and 0.1 wt% for CeO_2-ZrO_2), showing a clear reduction of the wear with respect to the neat base oil. The roughness (Ra) of the wear scar was also measured with an average uncertainty of 2 nm (Table 2) to analyse the anti-wear capacity of the nanolubricants and the possible wear mechanism produced by the nanoparticles. The presence of the nanoparticles generally produces an increase in the roughness of the wear pattern. This fact allows to confirm that the polishing effect produced by the nanoparticles is not the main mechanism that justifies the AW improvement for these nanolubricants, but a repair effect or a tribo-film formation can occur [45].

The reduction in the friction coefficient (COF) and the surface are obtained in this work when ZrO_2 or CeO_2-ZrO_2 are used as additives of PAO8, has been compared with those previously determined by Liñeira et al. [22,46] for PAO8 + (TiO_2-OA (coated with oleic acid), for PAO8 + $CaCO_3$ (uncoated) and PAO8 + CeF_3 (uncoated). As can be seen in Fig. 13a, the biggest reduction in the COF was obtained with the nanoparticles coated with oleic acid, TiO_2-OA, we must point out that in this case the PAO8 has been additivated with 0.35 wt% of TiO_2-OA but also with 0.20 wt% of oleic acid. For the uncoated nanoparticles ZrO_2 or CeO_2-ZrO_2 $CaCO_3$, the reductions are quite similar, around 13 % COF reduction, but the results are slightly worse with CeF_3. On the other hand, the biggest reductions obtained for the wear area in this work with ZrO_2 (73 %) are like those obtained previously [22] by using TiO_2-OA (76 %) as additive. For CeO_2-ZrO_2 the wear area reduction is better than those obtained with $CaCO_3$ and with CeF_3 (Fig. 13b).

To complete the analysis of the wear reduction mechanisms of ZrO_2 and CeO_2-ZrO_2, that can explain the improvement of the tribological performance, Raman microscopy studies were carried out. These measurements make possible both, to obtain a surface map within the wear tracks of the pins used, and to observe the distribution of the nanoparticles inside. Raman analysis was performed with a confocal Raman microscope at 532 nm wavelength for the wear tracks of the pins

Table 2
Average values for the surface roughness (Ra) of the wear track lubricated with the neat PAO8 and with each nanolubricant.

Lubricant	Ra/nm	Lubricant	Ra/nm	Lubricant	Ra/nm
PAO8	11	+0.1 wt% ZrO_2	31	+0.075 wt% CeO_2-ZrO_2	14
+0.05 wt% ZrO_2	17	+0.2 wt% ZrO_2	18	+0.1 wt% CeO_2-ZrO_2	21
+0.075 wt% ZrO_2	61	+0.05 wt% CeO_2-ZrO_2	14	+0.2 wt% CeO_2-ZrO_2	77

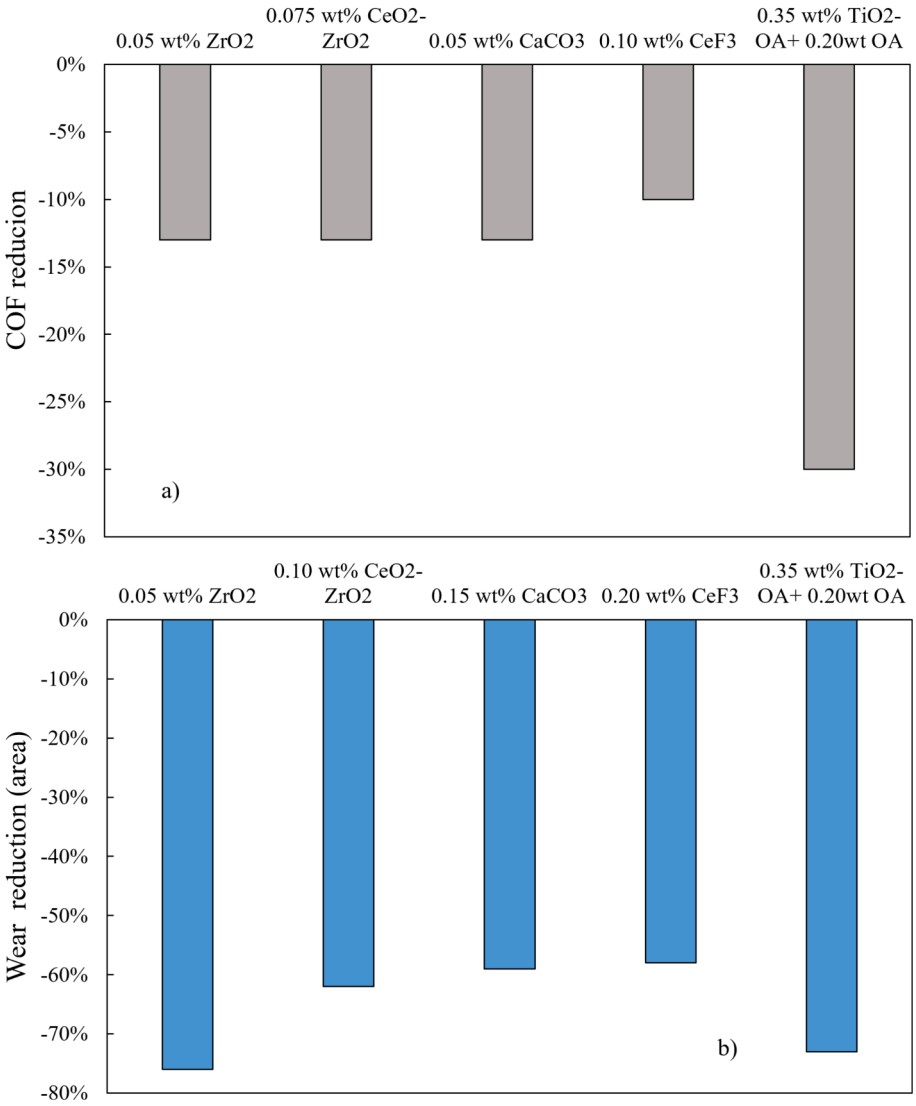

Fig. 13. Comparison of (a) the reduction in the COF and (b) the reduction in wear scar area versus previous results by Liñeira et al. [23,43] using the same base oil (PAO8).

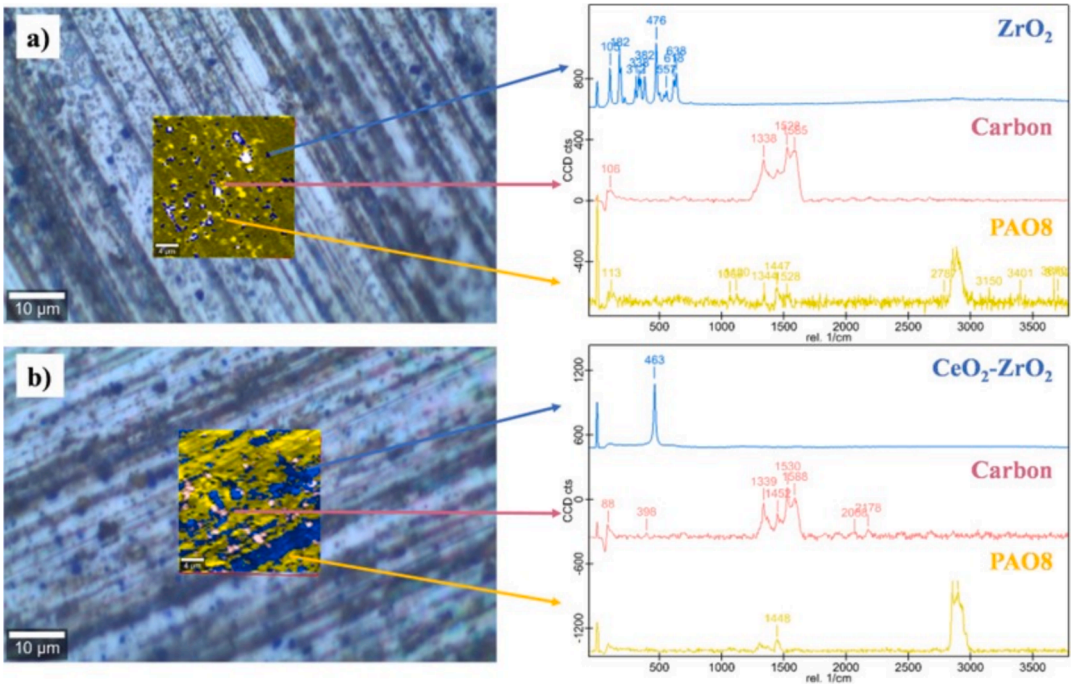

Fig. 14. Raman mapping analysis of the wear tracks of the pins lubricated with 0.05 wt% ZrO_2 (a) and with 0.1 wt% CeO_2-ZrO_2 (b) both in PAO8.

lubricated with the optimum concentrations of anti-wear capacity (0.05 wt% ZrO_2 and 0.1 wt% of CeO_2-ZrO_2). Raman spectra corresponding to neat PAO8 and to ZrO_2 and CeO_2-ZrO_2 nanoparticles were already presented in Fig. 1 and Fig. 4, respectively. As can be seen in Fig. 14, the grooves produced during the friction tests are clearly visible in the sliding direction along which an accumulation of PAO8 lubricant can be observed. In addition, the characteristic stripes of each nanoadditive have been detected in the wear tracks of the lubricated pins. Fig. 14a shows the analysis performed for the wear track generated on the steel surface of the contact lubricated with PAO8/ZrO_2 (0.05 wt%). Indeed, PAO8 is mostly spread over almost the entire surface of the contact lubricated steel and ZrO_2 nanoparticles (blue colour) are lodged along the wear track in the sliding direction.

As shows Fig. 14b, for the contact lubricated with PAO8/ CeO_2-ZrO_2 (0.1 wt%), a predominant presence of PAO8, (yellow colour) is observed, although the presence of the nanoadditive (CeO_2-ZrO_2) is also clear in the form of continuous tribo-films (blue colour). Traces of carbon have been detected on both surfaces analysed (pink colour). These carbon deposits are generated during friction tests due to the abrasion to which the steel is subjected, as previously pointed out by Nasser et al [47]. Therefore, the detection of both nanoadditives in the wear traces is evidence that the improved lubricating ability of the nanolubricants is due to the film-forming mechanism of the nanoparticles on the sliding surfaces, thus improving the tribological properties (friction and wear) of the base oil.

SEM observations, shown in Fig. 15, have been carried out at two different magnifications, 500 and 5000× for the steel pins lubricated with plain PAO8 base oil, with 0.05 wt% ZrO_2/PAO8 and with 0.1 wt% CeO_2-ZrO_2/PAO8 nanolubricants. In 500 X images (Fig. 15 a, c and e), the entire wear track generated on the steel pins lubricated can be observed. Thus, minor wear is revealed for the contact lubricated with 0.05 wt% ZrO_2, which coincides with the reported results in Table 1 and Fig. 12. The worn surface lubricated with ZrO_2-nanolubricant, i.e. Fig. 15(d), shows small pitting, which could be attributed to adhesive wear. Whereas when the contact is lubricated with CeO_2-ZrO_2 nanolubricant Fig. 15(f), deep elongated grooves along the sliding direction can be observed, which are formed as a product of abrasive wear [48]. This is consistent with the roughness measurements (Table 2). Thus, the type of wear produced varies depending on the nanoadditive used. The excellent anti-wear behaviour and friction effect using nanolubricants are closely related to the presence of ZrO_2 nanoparticles on the wear surface, which was verified by energy dispersive X-ray spectrometry (EDX). Table 3 shows the increase in elemental Zr content in the worn tracks lubricated with both nanolubricants. It can be stated that the Zr nanoparticles have been entrained on contact and interacted with the surface, leading to an improvement in the tribological behaviour of the base oil. However, the presence of Ce could not be detected in the contact. The most likely anti-wear mechanism of the nanoparticulate additive is the formation of a protective layer due to the welding of the nanoparticles onto the wear surface (tribosintering), which has been confirmed with Raman mapping (Fig. 14). In addition, the spherical morphology of the nanoparticles used can perform the rolling mechanism, whereby the nanoparticles act as nano-bearings between the contact surfaces [49].

5. Conclusions

In this work, experimental thermophysical and tribological

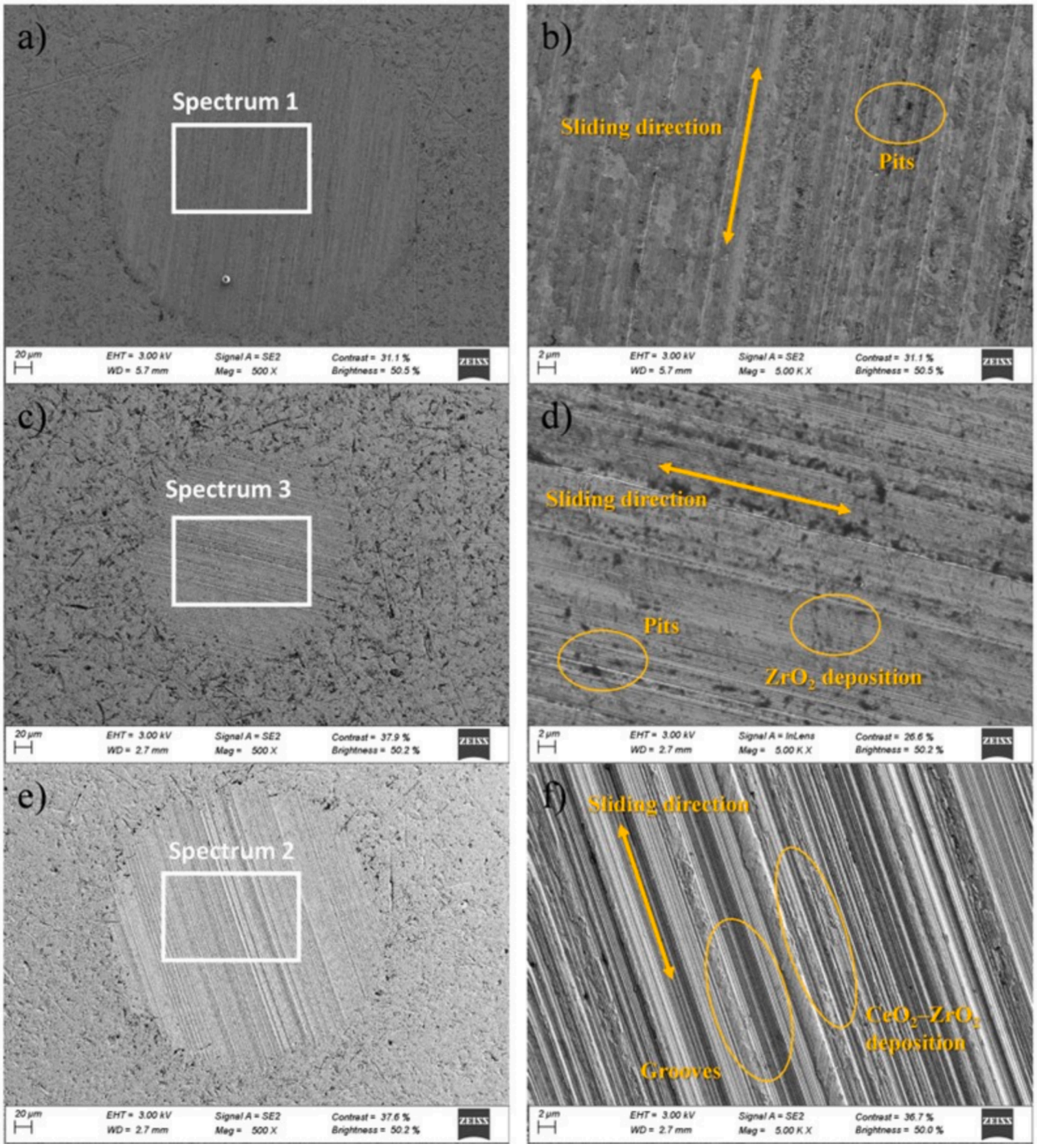

Fig. 15. SEM images inside of the wear scars on the steel pins from the test lubricated with: a) PAO8 (500 X), b) PAO8 (5000 X), c) PAO8 with 0.05 wt% ZrO_2 (500 X), d) PAO8 with 0.05 wt% ZrO_2 (5000 X), e) PAO8 with 0.1 wt% CeO_2-ZrO_2 (500 X) and f) PAO8 with 0.1 wt% CeO_2-ZrO_2 (5000 X).

Table 3
EDX analysis of worn surface of steel pins tested with PAO8 base oil, 0.1 wt% CeO_2-ZrO_2 and 0.05 wt% ZrO_2 nanolubricants.

Elemental composition	Steel AISI 52100/ Spectrum 1	0.1 wt% CeO_2-ZrO_2/Spectrum 3	0.05 wt% ZrO_2/ Spectrum 2
C	7.26	6.85	5.28
O	1.75	1.41	1.24
Mg	0.15	–	–
Al	0.60	0.18	0.12
Si	0.28	0.27	0.29
S	0.02	0.03	0.01
Cr	1.43	1.41	1.45
Mn	0.41	0.43	0.45
Fe	87.87	89.04	90.57
Zr	0.23	0.39	0.58
Total	100	100	100

properties were determined for PAO8 additivated with zirconia and hybrid ceria-zirconia nanoparticles at concentrations from 0.05 wt% to 0.2 wt%. The main findings of this study are:

- The presence of zirconia and hybrid ceria-zirconia does not affect the volumetric behaviour of the base oil, however, an increase in the viscosity up to 13 % is observed.
- The addition of ZrO_2 (0.05 wt%) or CeO_2-ZrO_2 (0.075 wt%) nanoparticles decreases the friction coefficient of PAO8 neat oil around 13 % under boundary lubrication conditions.
- ZrO_2 nanoadditives remove any abrasion or deformation of the surface: reduction of 66 % in the wear depth with respect to the neat base oil.
- The tribo-film formation and rolling effect produced by both types of spherical additives justify the improvement in the tribological behaviour.

CRediT authorship contribution statement

María J.G. Guimarey: Writing – review & editing, Writing – original draft, Validation, Resources, Methodology, Investigation, Conceptualization. **Arturo Castro Currás:** Methodology, Investigation. **José M. Liñeira Del Río:** Writing – review & editing, Writing – original draft, Validation, Methodology, Investigation. **María J.P. Comuñas:** Writing – review & editing, Supervision, Funding acquisition.

Declaration of competing interest

The authors declare that they have no known competing financial interests or personal relationships that could have appeared to influence the work reported in this paper.

Acknowledgements

This research is supported by projects PID2020-112846RB-C22 and ED431C 2024/06 funded by MCIN/AEI/10.13039/501100011033 and through the Xunta de Galicia, respectively. The authors would like to thank the use of RIAIDT-USC analytical facilities. Dr M.J.G.G. and Dr. J. M.L.dR are grateful for financial support through the grant reference ED481D 2023/016 from Xunta de Galicia (Spain) and the Margarita Salas programme, funded by MCIN/AEI/10.13039/501100011033 and "NextGenerationEU/PRTR", respectively.

Appendix A. Supplementary data

Supplementary data to this article can be found online at https://doi.org/10.1016/j.molliq.2025.127502.

Data availability

Data will be made available on request.

References

[1] Q. Qiao, F. Zhao, Z. Liu, S. Jiang, H. Hao, Cradle-to-gate greenhouse gas emissions of battery electric and internal combustion engine vehicles in China, Appl. Energy 204 (2017) 1399–1411, https://doi.org/10.1016/j.apenergy.2017.05.041.
[2] W.A.A. Mustafa, F. Dassenoy, M. Sarno, A. Senatore, A review on potentials and challenges of nanolubricants as promising lubricants for electric vehicles, Lubr. Sci. 34 (2022) 1–29, https://doi.org/10.1002/ls.1568.
[3] L.I. Farfan-Cabrera, Tribology of electric vehicles: A review of critical components, current state and future improvement trends, Tribol. Int. 138 (2019) 473–486, https://doi.org/10.1016/j.triboint.2019.06.029.
[4] O.A. Aguilar-Rosas, J.A. Alvis-Sánchez, B. Tormos, B.M. Marín-Santibáñez, J. Pérez-González, L.I. Farfan-Cabrera, Enhancement of low-viscosity synthetic oil using graphene nanoparticles as additives for enduring electrified tribological environments, Tribol. Int. 188 (2023) 108848, https://doi.org/10.1016/j.triboint.2023.108848.
[5] Y. Chen, S. Jha, A. Raut, W. Zhang, H. Liang, Performance Characteristics of Lubricants in Electric and Hybrid Vehicles: A Review of Current and Future Needs, Front. Mech. Eng. 6 (2020), https://doi.org/10.3389/fmech.2020.571464.
[6] M.B. Elinski, P. LaMascus, L. Zheng, A. Jackson, R.J. Wiacek, R.W. Carpick, Cooperativity Between Zirconium Dioxide Nanoparticles and Extreme Pressure Additives in Forming Protective Tribofilms: Toward Enabling Low Viscosity Lubricants, Tribol. Lett. 68 (2020) 107, https://doi.org/10.1007/s11249-020-01346-1.
[7] Y. Kwak, C. Cleveland, A. Adhvaryu, X. Fang, S. Hurley, T. Adachi, Understanding Base Oils and Lubricants for Electric Drivetrain Applications, SAE International (2019).
[8] L.R. Rudnick, Polyalphaolefins, in: L.R.E. Rudnick (Ed.), Synthetics, Mineral Oils, and Bio-Based Lubricants: Chemistry and Technology, CRC Press, 2020.
[9] R. Benda, J. Bullen, A. Plomer, Synthetics basics: Polyalphaolefins — base fluids for high-performance lubricants, J. Synth. Lubr. 13 (1996) 41–57, https://doi.org/10.1002/jsl.3000130105.
[10] Z.A.A.A. Ali, A.M. Takhakh, M. Al-Waily, A review of use of nanoparticle additives in lubricants to improve its tribological properties, Mater. Today: Proc. 52 (2022) 1442–1450, https://doi.org/10.1016/j.matpr.2021.11.193.
[11] A. Ashraf, W.K. Shafi, M.I. Ul Haq, A. Raina, Dispersion stability of nano additives in lubricating oils – an overview of mechanisms, theories and methodologies, Tribol. – Mater. Surf. Interfaces 16 (2022) 34–56, https://doi.org/10.1080/17515831.2021.1981720.
[12] F. Dassenoy, Nanoparticles as Additives for the Development of High Performance and Environmentally Friendly Engine Lubricants, Tribol. Online 14 (2019) 5, https://doi.org/10.2474/trol.14.237.
[13] I.E. Uflyand, V.A. Zhinzhilo, V.E. Burlakova, Metal-containing nanomaterials as lubricant additives: State-of-the-art and future development, Friction 7 (2019) 93–116, https://doi.org/10.1007/s40544-019-0261-y.
[14] M.K.A. Ali, X. Hou, M.A.A. Abdelkareem, Anti-wear properties evaluation of frictional sliding interfaces in automobile engines lubricated by copper/graphene nanolubricants, Friction 8 (2020) 905–916, https://doi.org/10.1007/s40544-019-0308-0.
[15] J. Wang, W. Zhuang, W. Liang, T. Yan, T. Li, L. Zhang, S. Li, Inorganic nanomaterial lubricant additives for base fluids, to improve tribological performance: Recent developments, Friction 10 (2022) 645–676, https://doi.org/10.1007/s40544-021-0511-7.
[16] M. Kalin, J. Kogovšek, M. Remškar, Mechanisms and improvements in the friction and wear behavior using MoS_2 nanotubes as potential oil additives, Wear 280–281 (2012) 36–45, https://doi.org/10.1016/j.wear.2012.01.011.
[17] R. Chou, A.H. Battez, J.J. Cabello, J.L. Viesca, A. Osorio, A. Sagastume, Tribological behavior of polyalphaolefin with the addition of nickel nanoparticles, Tribol. Int. 43 (2010) 2327–2332, https://doi.org/10.1016/j.triboint.2010.08.006.
[18] A. Hernandez Battez, J.E. Fernandez Rico, A. Navas Arias, J.L. Viesca Rodriguez, R. Chou Rodriguez, J.M. Diaz Fernandez, The tribological behaviour of ZnO nanoparticles as an additive to PAO6, Wear 261 (2006) 256–263, https://doi.org/10.1016/j.wear.2005.10.001.
[19] S.M. Alves, B.S. Barros, M.F. Trajano, K.S.B. Ribeiro, E. Moura, Tribological behavior of vegetable oil-based lubricants with nanoparticles of oxides in boundary lubrication conditions, Tribol. Int. 65 (2013) 28–36, https://doi.org/10.1016/j.triboint.2013.03.027.
[20] F. Mariño, J.M. Liñeira del Río, D.E.P. Gonçalves, J.H.O. Seabra, E.R. López, J. Fernández, Effect of the addition of coated SiO_2 nanoparticles on the tribological behavior of a low-viscosity polyalphaolefin base oil, Wear 530–531 (2023) 205025, https://doi.org/10.1016/j.wear.2023.205025.
[21] F. Mariño, E.R. López, Á. Arnosa, M.A. González Gómez, Y. Piñeiro, J. Rivas, C. Alvarez-Lorenzo, J. Fernández, ZnO nanoparticles coated with oleic acid as additives for a polyalphaolefin lubricant, J. Mol. Liq. 348 (2022) 118401, https://doi.org/10.1016/j.molliq.2021.118401.
[22] J.M. Liñeira del Río, F. Mariño, E.R. López, D.E.P. Gonçalves, J.H.O. Seabra, J. Fernández, Tribological enhancement of potential electric vehicle lubricants using coated TiO_2 nanoparticles as additives, J. Mol. Liq. 371 (2023) 121097, https://doi.org/10.1016/j.molliq.2022.121097.

[23] C. Tao, B. Wang, G.C. Barber, J.D. Schall, H. Lan, Tribological behaviour of SnO_2 nanoparticles as an oil additive on brass, Lubr. Sci. 30 (2018) 247–255, https://doi.org/10.1002/ls.1416.
[24] M.J.G. Guimarey, M.J.P. Comuñas, E.R. López, A. Amigo, J. Fernández, Thermophysical properties of polyalphaolefin oil modified with nanoadditives, J. Chem. Thermodyn. 131 (2019) 192–205, https://doi.org/10.1016/j.jct.2018.10.035.
[25] A. Hernández Battez, R. González, J.L. Viesca, J.E. Fernández, J.M. Díaz Fernández, A. Machado, R. Chou, J. Riba, CuO, ZrO_2 and ZnO nanoparticles as antiwear additive in oil lubricants, Wear 265 (2008) 422–428, https://doi.org/10.1016/j.wear.2007.11.013.
[26] I. Lahouij, B. Gould, N. Demas, A. Greco, Z. Chen, G.D. Cooper, A. Jackson, R. W. Carpick, Inhibition of Micro-pitting by Tribofilm-Forming ZrO_2 Nanocrystal Lubricant Additives: A Micro-pitting Rig and Transmission Electron Microscope Study, Tribol. Lett. 70 (2022) 13, https://doi.org/10.1007/s11249-021-01555-2.
[27] S.J. Thrush, A.S. Comfort, J.S. Dusenbury, X. Han, X. Wang, H. Qu, G.C. Barber, Study of pressure dependence on sinterable zirconia nanoparticle tribofilm growth, Tribol. Int. 154 (2021) 106683, https://doi.org/10.1016/j.triboint.2020.106683.
[28] J.T. Philip, C.P. Koshy, M.D. Mathew, Advanced characterization of precipitation synthesized ceria and ceria-zirconia hybrid nanoparticles, Mater. Res. Express 6 (2019) 1150e1151, https://doi.org/10.1088/2053-1591/ab4fd5.
[29] C. Li, X. Wang, Q. Zhang, X. Tan, Y. Liu, H. Li, H. Liu, E. Hu, X. Hu, Synthesis, characterization and tribological performances of nano-CeO_2/biodiesel carbon soot composites as a novel lubricant additive in polyalphaolefin, J. Ind. Eng. Chem. 126 (2023) 432–443, https://doi.org/10.1016/j.jiec.2023.06.031.
[30] L. Wu, X. Lei, Y. Zhang, S. Zhang, G. Yang, P. Zhang, The Tribological Mechanism of Cerium Oxide Nanoparticles as Lubricant Additive of Poly-Alpha Olefin, Tribol. Lett. 68 (2020) 101, https://doi.org/10.1007/s11249-020-01340-7.
[31] M.K.A. Ali, H. Xianjun, Exploring the lubrication mechanism of CeO_2 nanoparticles dispersed in engine oil by bis(2-ethylhexyl) phosphate as a novel antiwear additive, Tribol. Int. 165 (2022) 107321, https://doi.org/10.1016/j.triboint.2021.107321.
[32] M. Praveena, K. Guha, A. Ravishankar, S.K. Biswas, C.D. Bain, V. Jayaram, Total internal reflection Raman spectroscopy of poly(alpha-olefin) oils in a lubricated contact, RSC Adv. 4 (2014) 22205–22213, https://doi.org/10.1039/C4RA02261K.
[33] H. Okubo, C. Tadokoro, Y. Hirata, S. Sasaki, In Situ Raman Observation of the Graphitization Process of Tetrahedral Amorphous Carbon Diamond-Like Carbon under Boundary Lubrication in Poly-Alpha-Olefin with an Organic Friction Modifier, Tribol. Online 12 (2017) 229–237, https://doi.org/10.2474/trol.12.229.
[34] M. Yashima, T. Hirose, S. Katano, Y. Suzuki, M. Kakihana, M. Yoshimura, Structural changes of ZrO_2-CeO_2 solid solutions around the monoclinic-tetragonal phase boundary, Phys. Rev. B, Condensed Matter 51 (1995) 8018–8025, https://doi.org/10.1103/physrevb.51.8018.
[35] S.N. Basahel, T.T. Ali, M. Mokhtar, K. Narasimharao, Influence of crystal structure of nanosized ZrO_2 on photocatalytic degradation of methyl orange, Nanoscale Res. Lett. 10 (2015) 73, https://doi.org/10.1186/s11671-015-0780-z.
[36] K. Periyasamy, V.T. Aswathy, V.A. kumar, M. Manikandan, R. Shukla, A.K. Tyagi, T. Raja, An efficient robust fluorite $CeZrO_{4-\delta}$ oxide catalyst for the eco-benign synthesis of styrene, RSC Adv. 5 (2015) 3619–3626, https://doi.org/10.1039/C4RA12355G.
[37] F.M. Gaciño, T. Regueira, L. Lugo, M.J.P. Comuñas, J. Fernández, Influence of Molecular Structure on Densities and Viscosities of Several Ionic Liquids, J. Chem. Eng. Data 56 (2011) 4984–4999, https://doi.org/10.1021/je200883w.
[38] S.M. Hsu, R.S. Gates, Boundary lubrication and boundary lubricating films, in: B. Bhushan (Ed.), Modern Tribology Handbook, CRC Press, Boca Raton, 2000.
[39] K. Holmberg, P. Andersson, A. Erdemir, Global energy consumption due to friction in passenger cars, Tribol. Int. 47 (2012) 221–234, https://doi.org/10.1016/j.triboint.2011.11.022.
[40] F. Chiñas-Castillo, H.A. Spikes, Mechanism of Action of Colloidal Solid Dispersions, J. Tribol. 125 (2003) 552–557, https://doi.org/10.1115/1.1537752.
[41] M.J.G. Guimarey, S. Karunarathne, C.R. Ratwani, J.L. Viesca, A.H. Battez, A. M. Abdelkader, 2D mica as a new additive for nanolubricants with high tribological performance, Tribol. Int. 200 (2024) 110075, https://doi.org/10.1016/j.triboint.2024.110075.
[42] N.N.M. Zawawi, W.H. Azmi, A.A.M. Redhwan, M.Z. Sharif, Coefficient of friction and wear rate effects of different composite nanolubricant concentrations on Aluminium 2024 plate, IOP Conf. Ser. Mater. Sci. Eng. 257 (2017) 012065, https://doi.org/10.1088/1757-899X/257/1/012065.
[43] L. Hao, Z. Wang, G. Zhang, Y. Zhao, Q. Duan, Z. Wang, Y. Chen, T. Li, Tribological evaluation and lubrication mechanisms of nanoparticles enhanced lubricants in cold rolling, Mech. Ind. 21 (2020) 108, https://doi.org/10.1051/meca/2019085.
[44] T. Kulkarni, B. Toksha, A. Autee, Optimizing nanoparticle attributes for enhanced anti-wear performance in nano-lubricants, J. Appl. Eng. Sci. 71 (2024) 30, https://doi.org/10.1186/s44147-024-00374-1.
[45] U. Maurya, V. Vasu, D. Kashinath, Three-way compatibility study among Nanoparticles, Ionic Liquid, and Dispersant for potential in lubricant formulation, Mater. Today: Proc. 59 (2022) 1651–1658, https://doi.org/10.1016/j.matpr.2022.03.329.
[46] J.M. Liñeira del Río, A. Alba, M.J.G. Guimarey, J.I. Prado, A. Amigo, J. Fernández, Surface tension, wettability and tribological properties of a low viscosity oil using $CaCO_3$ and CeF_3 nanoparticles as additives, J. Mol. Liq. 391 (2023) 123188, https://doi.org/10.1016/j.molliq.2023.123188.
[47] K.I. Nasser, J.M. Liñeira del Río, E.R. López, J. Fernández, Synergistic effects of hexagonal boron nitride nanoparticles and phosphonium ionic liquids as hybrid lubricant additives, J. Mol. Liq. 311 (2020) 113343, https://doi.org/10.1016/j.molliq.2020.113343.
[48] U. Maurya, V. Vasu, Boehmite nanoparticles for potential enhancement of tribological performance of lubricants, Wear 498–499 (2022) 204311, https://doi.org/10.1016/j.wear.2022.204311.
[49] W. Dai, B. Kheireddin, H. Gao, H. Liang, Roles of nanoparticles in oil lubrication, Tribol. Int. 102 (2016) 88–98, https://doi.org/10.1016/j.triboint.2016.05.020.